Author post-print version. Published in *IEEE. Trans. Appl. Supercond*. 29 (2019) 6801109

Magnetic shielding of open and semi-closed bulk superconductor tubes: the role of a cap

Laurent Wéra, Jean-François Fagnard, Kevin Hogan, Benoît Vanderheyden, Devendra Kumar Namburi, Yunhua Shi, David A. Cardwell and Philippe Vanderbemden

***Abstract*—In this paper we investigate the magnetic shielding of hollow and semi-closed bulk superconducting tubes at 77 K. We first consider the properties of a commercial Bi-2223 tube closed by a disk-shaped cap placed against its extremity. The results are compared to those obtained on a bulk large grain Y-Ba-Cu-O (YBCO) tube produced by buffer-aided top seeded melt growth. In this process, the disk-shaped pellet and the tubular sample are grown together, resulting in a tube naturally closed at one extremity. The field to be shielded is either parallel or perpendicular to the main axis of the tube. The experimental results are compared with the results of finite element numerical modelling carried out either in 2D (for the axial configuration) or 3D (for the transverse configuration). In the axial configuration, the results show that the shielded volume can be enhanced easily by increasing the thickness of the cap. In the transverse configuration, the results show the critical role played by the superconducting current loops flowing between the tube and the cap for magnetic shielding. If the tube and the cap are separated by a non-superconducting joint or air gap, the presence of a cap leads to only a small improvement of the transverse shielding factor, even for a configuration where the gap between the cap and the tube contains a 90° bend. The cap leads to a significant increase in the transverse shielding when the cap and the tube are naturally grown in the same process, i.e. made of a continuous superconducting material. The experimental results can be reproduced qualitatively by 3D numerical modelling.**

***Index Terms*—Magnetic shielding, Bulk high-temperature superconductors.**

I. Introduction

ONE promising application of hollow, bulk superconductors is low frequency magnetic shielding. Superconductors allow an ultra-low magnetic field background to be achieved in several applications ranging from biomedical engineering to high-sensitivity instrumentation [1-4]. Unlike conventional high permeability ferromagnetic materials, however, which exhibit a relatively low saturation magnetization (e.g. $\mu_0 M_{sat} \sim$ 0.7 T for mu-metal [5]), superconductors do not suffer from this limitation. They are, therefore, well suited for shielding particle beams and creating a field-free region within a high external field [6-8]. Shielding magnetic flux densities above 1 tesla can be achieved by hollow bulk superconductors of various compositions, e.g. $Bi_2Sr_2CaCu_2O_8$ (Bi-2212) [9], MgB_2 [10-12] or $YBa_2Cu_3O_7$ (YBCO) [13]. Several studies have also been carried out on $Bi_2Sr_2Ca_2Cu_3O_{10}$ (Bi-2223) [14,15] which can be grown in the shape of large vessels [1], and promising shielding properties were demonstrated recently with $GdBa_2Cu_3O_7$ single domains [16]. Shields made of bulk superconductors can be hybridized conveniently with ferromagnetic materials [17,18] or with coated conductors [15] to take advantage of the additional shielding effect provided by these materials [19-21] or to achieve shielding without distortion of external flux lines (so-called "cloaking") [7,22].

One of the main characteristics of superconducting shields is that the field attenuation is due to the presence of macroscopic current loops flowing at the periphery of the shield. This feature, therefore, makes them sensitive to the presence of slits or non-superconducting joints in the shield construction [23,24]. Taking into account that growing large-size bulk superconductors is notoriously challenging [25], understanding how to increase the shielded volume inside a shield of given dimensions is of fundamental importance to the development of a practical device. The beneficial effects of a cap placed against the opening of a bulk type-II superconducting tube were studied numerically one decade ago [26] using a semi-analytical approach based on the Brandt algorithm [27] in a 2D axisymmetric configuration. Some of the results of this study were extended and confirmed experimentally on Bi-2223 superconducting shields of various aspect ratios subjected to an axial magnetic field [28]. These results confirmed the major influence of the aspect ratio of the shield on the shielded volume. In a simple geometry where the tube is subjected to an axial field H_{app} (as shown schematically in Fig. 1), the quality of a joint perpendicular to the applied field has no effect on the superconducting currents, and hence on magnetic shielding. In practice, however, the stray field to be shielded is rarely uniform and often has a small transverse field component [29].

This work was supported in part by the *Communauté Française de Belgique* under Grant ARC 11-16/03. K Hogan is holder of a research grant from the *Fonds pour la formation à la Recherche dans l'Industrie et dans l'Agriculture* (FRIA). The authors would like to thank the financial support from the EPSRC project EP/P00962X/1.

L. Wéra, J.-F. Fagnard, K. Hogan B. Vanderheyden and P. Vanderbemden are with the SUPRATECS group, "Montefiore" research unit, in the Department of Electrical Engineering and Computer Science at the University of Liège, Belgium (corresponding author: Philippe.Vanderbemden@ulg.ac.be). L. Wéra is on leave for AMOS (Advanced Mechanical and Optical Systems), Belgium. D. K. Namburi, Y. Shi and D. A. Cardwell and are with the Bulk Superconductivity Group in the Department of Engineering at the University of Cambridge, UK.

The suitability of any tube termination, therefore, needs to be examined in the transverse configuration. This can be done using both experiment and modelling for analyzing the properties of bulk superconductors [30,31].

The purpose of the present work is to investigate and clarify the advantages of placing a cap against a bulk, type-II superconducting tube, particularly in the transverse configuration. The geometries studied in the present work are shown schematically in Fig. 1. A hollow tube ("open") was used as a reference, and the three other configurations were closed on one side. In the so-called "closed" geometry, a superconducting disk of the same diameter as the outer diameter of the tube was placed against one opening, with a non-superconducting air gap between the tube and the cap. The "adjusted" geometry refers to a hollow cylinder where the inner part of the tube wall is machined to half of its thickness at one extremity, such that a cap can fit inside the tube. In this case, the diameter of the cap is the average of the inner and outer diameters of the tube. The difference with respect to the "closed" geometry is that the non-superconducting air gap is not perpendicular to the axis of the tube but contains a 90° bend. In the final configuration, we consider a tube in which the wall and the cap are fabricated in the same process, such that both are "fused" together, resulting in a tube naturally closed at one extremity. Such tubes were engineered recently by a Buffer-Aided Top Seeded Melt Growth (BA-TSMG) fabrication process [32,33] and exhibited remarkable shielding performances under axial magnetic fields [13]. Their properties are investigated under a transverse field in the present work.

II. Experiment

Two kinds of superconductors were studied experimentally. The investigations for the "open", "closed" and "adjusted" configurations were carried out on commercial Bi-2223 hollow cylinders supplied by CAN superconductors [34]. The superconducting disk covering the extremity of the tube was made of the same material. The gap between the cap and the tube in the "closed" and "adjusted" configurations was made as small as possible (~ 0.1 mm). The "fused" sample consisted of bulk, large grain YBCO fabricated by the Buffer-Aided Top Seeded Melt Growth [32,33]. Details of the fabrication process can be found in [13]. The resulting tube is closed at one extremity by a pellet containing the seed used for melt processing. The geometric dimensions of the cylindrical samples and of the caps are summarized in Table I.

Magnetic shielding measurements were carried out at liquid nitrogen temperature (77 K). The tubes were subjected to a uniform quasi-static (dc) magnetic field produced by a solenoidal coil of 450 mm in length and 200 mm in diameter. The field was applied either along the axis of the tube (axial configuration) or perpendicular to it (transverse configuration). The magnetic field was ramped at a constant sweep rate of 0.1 mT/s and the magnetic flux density inside the tube was recorded using a 3-axis Hall probe (*Arepoc* Axis-3H), which could be moved along the axis of the tube. In this study, the component of the magnetic flux density parallel to the applied field was recorded either at the center of the tube or at its extremity, i.e. against the cap for configurations (b) to (d) in Fig. 1.

III. Modelling

Finite element modelling was performed using an A-ϕ formulation, in which Maxwell equations were solved for two independent variables, the vector potential **A** and the scalar potential ϕ [35-37], using open-source software GetDP developed at the Applied and Computational Electromagnetics laboratory of the University of Liege [38]. Details concerning the implementation of this code can be found in [37,38].

Modelling was carried out first in an axisymmetric configuration (2D), for a geometry corresponding to that of the commercial Bi-2223 tube. The geometric dimensions of the samples used in 2D modelling are summarized in Table II (left column). For the "closed" and "adjusted" configurations the non-superconducting joint between the cap and the tube was taken to 0 mm. The superconducting properties were modelled using an *E-J* power law $E(J) = E_c(J/J_c)^n$. According to previous experiments carried out on the same material at $T = 77$ K [14], we use a n-value = 30 and the field-dependence of the critical current density J_c is assumed to follow Kim's law, i.e.

$$J_c(B) = J_{c0}\left(1 + \frac{B}{B_1}\right)^{-1} \qquad (1)$$

with $J_{c0} = 900$ A/cm² and $B_1 = 3$ mT. The nominal thickness of the disk-shaped cap e_0 is 2 mm. According to independent experiments carried out on the disk-shaped materials, slightly different critical current density parameters were used for the cap, i.e. $J_{c0} = J_{c0}^* = 750$ A/cm² and $B_1 = 5$ mT. In order to investigate the influence of the cap geometry and properties, different thicknesses from (e_0/2) to (4e_0) and different J_{c0} from (J_{c0}^*/2) to (4J_{c0}^*) were used. In this latter case, the value of the parameter B_1 was kept unchanged.

Modelling was carried out in 3D to study the different transverse configurations shown in Fig. 1. We chose to model a short cylinder (height = 30 mm, outer diameter = 26 mm) with an aspect ratio close to that of the "fused" sample, given that the 3D modelling requires a significant number of elements (in addition to a rather long computation time). The geometric dimensions of the samples and caps used in 3D modelling are summarized in Table II (right column). The non-superconducting joint between the cap and the tube for the "closed" and "adjusted" configurations was modelled by a 1 mm air gap due to the necessity to mesh the air part with a sufficient resolution. The external diameter of the cap was either 26 mm ("closed" and "fused" configuration) or 21 mm ("adjusted" configuration), its thickness was 2 mm. Using these dimensions, the aspect ratio (length/average diameter) of the modelled sample was ~ 1.3, which was very close to that (~ 1.28) of the YBCO material fabricated by the Buffer-Aided Top Seeded Melt Growth. According to previous experiments carried out on the same material at $T = 77$ K, the critical current

density of all superconducting components is assumed to be field-independent and equal to 1000 A/cm². The critical exponent was taken to $n = 25$, in agreement with the usual range on n-values used for bulk melt-textured YBCO materials at liquid nitrogen temperature [30,37].

IV. Results and Discussion

The parameter used to assess the shielding efficiency is the shielding factor (SF), defined as the ratio between the applied field strength $B_{app} = \mu_0 H_{app}$ and the magnetic flux density B_{in} measured inside the superconducting shield along the direction of B_{app}, i.e. $SF = B_{app} / B_{in}$.

A. Axial configuration

We first examine the experimental data obtained for the long tube (Bi-2223) for the "open", "closed" and "adjusted" configurations. Figure 2a shows the shielding factor as a function of the axial magnetic field. For the open tube, the shielding factor at the center of the tube exceeds 10^3 at low field and decreases gradually with increasing field, to reach 10^2 for $\mu_0 H_{app} \sim 6.9$ mT. This value can be taken as the "limit" or "threshold" induction B_{lim}, above which shielding becomes weakly effective. The shielding factor in the vicinity of the open extremity is strongly suppressed compared to that in the center, e.g. at 1 mT the shielding factor is only 4.2. This behavior is expected due to penetration of the field through the open end [26]. The shielding properties at the center of the tube are almost unaffected by the presence of the cap in the "closed" configuration (the shielding factor at the center of the "adjusted" configuration was not measured). As an example, the magnetic field strengths at which $SF = 10$ at the center are $\mu_0 H_{app} \sim 7.4$ mT for both "open" and "closed" configurations. The presence of the cap leads to a significant improvement of the shielding factor at the extremity for both "closed" and "adjusted" geometries (blue and green lines with open symbols in Fig. 2a). This yields a significant increase of the volume in which strong magnetic shielding (e.g. $SF > 10^2$) is observed.

2D numerical modelling of the shielding factor for the "open" and "closed" configurations was carried out in the same range of applied fields as for the experiment. Results are plotted in Fig. 2b and can be compared quantitatively to those plotted in Fig. 2a. At the center of the tube, the magnetic field strengths at which $SF = 10$ are 7.51 mT and 7.56 mT for the "open" and "closed" configurations respectively, against ~ 7.4 mT for the experiment. At the covered extremity of the closed tube, the modelled SF is equal to 10 for an applied field strength of 11.65 mT, against 11.5 mT for the experiment. At the open extremity (black open circles in Fig. 2), the modelled shielding factor at 1 mT is 4.37, against 4.2 for the experiment. The nice quantitative agreement between the model and the experiment gives confidence that the 2D model can be used to investigate further other parameters or geometric configurations. As an example, the 2D model was run under an applied field strength of 7 mT, i.e. slightly above $B_{lim} \sim 6.9$ mT defined earlier, in order to visualize the improvement of the shielding volume in a regime where the distribution of magnetic flux density in the volume delimited by the shield is inhomogeneous. Results are shown in Fig. 3, where the scale is defined so that the white zone in the tube corresponds to a shielding factor taken arbitrarily to be $SF > 20$, i.e. $|B| < 0.35$ mT. This white zone defines the shape of the shielded volume. The "open" configuration displayed on the left of the figure serves as reference. The configuration referring to the experiment corresponds to the nominal value of both the critical current ($J_{c0} = J_{c0}^*$) and the cap thickness (e_0), as shown in the dashed frame of Fig. 3.

The numerical results indicate clearly the beneficial effect of the cap and show that the increase of the shielded volume due to the cap occurs both in the central region of the tube and in the vicinity of the cap. The field concentration near the extremity of the tube is caused by the expected bending of the magnetic field lines around the cap [28]. In the present case, where the superconducting material is characterized by a strong $J_c(B)$ dependence, the field concentration affects the local critical current density, resulting in a reduced efficiency of the cap, compared to what could be expected for a constant J_c.

It is of interest to investigate how the shielded volume varies when the critical current density of the cap is adjusted (from half the nominal value to 4 times the nominal value), given that the cap and the tube itself can be constructed of different materials. Results are shown in the upper graphs of Fig. 3. It can be seen that a significant extension of the shielded zone can be achieved when J_c is multiplied by a factor of 4. Knowing that, according to the Bean model with a constant J_c [39], the full penetration field of an infinite slab of thickness e in parallel field is proportional to the product ($J_c.e$), further modelling was carried out for different thicknesses, and the results are shown in the lower graphs of Fig. 3. Remarkably, an increase of the shielded volume similar to that caused by a larger J_c is also observed, although the applied field is not parallel to the largest face of the cap and the critical current density is field dependent. The shielded volume for $4e_0$ is even found to be slightly larger than for $4J_{c0}$. This phenomenon might be due to the fact that the field concentration zone (where J_c is depressed) is more distant from the interior zone of the tube for a larger cap. This is dependent, however, on the exact $J_c(B)$ relationship for both the cap and the tube, on the strength of the applied field (in the present case $\mu_0 H_{app} > B_{lim}$) as well as the arbitrarily chosen value for delimiting the shielded volume.

It can be concluded from the above results that a simple cap placed against the sample is extremely helpful in improving the shielded volume and that this volume can be further increased by employing a cap with either a higher J_c or greater thickness. The latter seems to be a more practical solution, since a thicker cap can be replaced by several caps that can be stacked above each other.

B. Transverse configuration

Now we turn to the configuration where the applied field is perpendicular to the tube axis. Results obtained for the "open", "closed" and "adjusted" geometries are shown in Fig. 4. Firstly, the shielding factor values measured at the center of the tube (solid symbols) are smaller than those plotted in Fig. 2. The value of B_{lim} defined for a $SF = 10^2$ in this case is ~ 4.5 mT, against 6.9 mT in axial field. Taking into account the "eye shape" of the flux front inside the wall of a type-II infinite tube

in the transverse configuration, it is possible to determine [14] an approximate relation between the two quantities, i.e.:

$$\frac{B_{lim}(axial)}{B_{lim}(transverse)} \approx 1 + \frac{R_{in}}{R_{out}}, \qquad (2)$$

where R_{in} and R_{out} are the inner and outer radii of the tube, respectively. This procedure gives an approximate ratio of ~ 1.85, compared to (6.9/4.5) ~ 1.53 observed experimentally. The difference can be attributed to the finite height of the tube as well as the field-dependent $J_c(B)$. All shielding factors measured at the extremity of the tube (the open symbols in Fig. 4) are smaller than those measured at the center. The significant reduction of shielding factor can be attributed to the presence of the air gap, which is now parallel to the main direction of the applied field. It can be noticed, however, that the cap placed against the opening ("closed" configuration) leads to a small increase of the shielding factor, which is further improved (albeit slightly) in the "adjusted" configuration. The results presented in Fig. 4, therefore, show that the presence of the right angle in the air gap introduces a small beneficial effect in the transverse configuration, but only at low magnetic fields.

We now consider the shielding factor of the "fused" sample subjected to a transverse field (Fig. 5). Unlike the behavior depicted in Fig. 4, the shielding factor measured near the covered extremity (open symbols) is increased by a factor ranging between ~ 3 and ~ 7 compared to its value at the center of the tube (solid symbols), e.g. at $\mu_0 H_{app}$ ~ 50 mT one has *SF*(extremity) / *SF*(center) ~ 4. This result shows the significant improvement introduced by the cap in the transverse configuration, and gives indirect evidence of the superconducting nature of the medium joining the tube and the cap for this material.

3D numerical modelling was used to develop a better understanding of the shielding current distribution in the configurations studied above. The geometry used for modelling is shown in Fig. 1, and the value of the geometric and superconducting parameters are given in Table II. Fig. 6 shows the shielding factor modelled for the 4 configurations studied. For the open tube (black circles), we notice first that the shielding factor at the center of the tube is much smaller than those measured experimentally for the long Bi-2223 sample. This is explained by the small aspect ratio of the modelled cylinder, and penetration through the open ends of the tube. The presence of a cap with a small air gap ("closed" and "adjusted" configurations) has almost no effect on the *SF* values determined at the center. For the "closed" and "adjusted" configurations, the shielding factor at the extremity of the tube is slightly higher than for the "open" sample, as also observed in the experimental data on the Bi-2223 material (Fig. 4). The behavior of the "fused" sample is markedly different from the others: the shielding factor at the center of the cylinder at the closed extremity is increased significantly, with better shielding observed near the cap, as also observed in the experimental data for the "fused" sample (Fig. 5).

Results of the 3D modelling can be compared to rough analytical estimations. First, we consider the maximum shielding factor of the studied samples. At very low magnetic field, the field penetration depth is extremely small relative to the wall thickness and it seems justified to compare the shielding factor to that of a type-I superconductor of the same dimensions. For a short cylinder of inner radius R_{in} and height h subjected to a transverse field, the theoretical shielding factor along the axis at a distance z from the center can be estimated by [40]:

$$SF(trans) \approx exp\left[1.84\left(\frac{h}{2} - z\right)/R_{in}\right]. \qquad (3)$$

Taking an average radius $R = 11.5$ mm and a height $h = 30$ mm, we obtain a shielding factor of 11 at the center of the open cylinder (black star in Fig. 6) which is quite close to that modelled for the first 3 configurations, i.e. when there is an air gap between the cap and the tube. For the "fused" sample, the shielding factor at the closed extremity can be estimated by considering the *SF* at the center of a cylinder of twice its length ($h = 60$ mm). From Eq. (3), we obtain a shielding factor of 121 (red star in Fig. 6), which is reasonably close to that observed for the values modelled at low magnetic field.

An additional feature that can be observed in Fig. 6 is the rapid decrease of the modelled shielding factor against the extremity of the "fused" sample when the applied magnetic field strength is around ~ 20 mT. Given the J_c and the wall thickness of the modelled geometry ($d = 3$ mm), the full penetration field estimated from the Bean model for an infinitely long sample in the axial configuration would be $\mu_0 J_c d \approx 38$ mT. According to Eq. (2), this value should be divided by the factor $(1 + R_{in}/R_{out}) \approx 1.77$ in the transverse configuration, giving a full penetration field of about 21.3 mT if the sample was infinite. Remarkably, this corresponds to the value around which the shielding factor in the "fused" sample (next to the cap) collapses, giving evidence that the relevant penetration mechanism at this field level is likely to be through the walls of the tube. When comparing the values of the 3D modelled shielding factor for the "fused" sample (orange triangles in figure 6) to the experimental data (figure 5), the two following differences can be noticed: (i) at low field (e.g. 3 mT), the modelled shielding factor is found to be higher than the experimental one and (ii) at higher field (e.g. 20 mT) the opposite phenomenon is observed. The exact reason for this behavior remains unknown and might be attributed to an inhomogeneous J_c of the bulk sample. What is clear is that the stronger field-dependence observed for the modelled shielding factor is not related to any field-dependence of the critical current $J_c(B)$ since a constant J_c was assumed for the modelling.

Finally, Fig. 7 shows the distribution of the current density for $B_{app} = 30$ mT, i.e. in the fully penetrated regime. For the "closed" sample, there is no current flowing between the cap and the cylinder. Shielding currents in the cylinder (Fig. 7a) and in the plane orthogonal to the applied field are similar to those observed in hollow cylinders and bulk pellets in transverse field configuration, but here brought next to each other. In this situation, the cylinder and the cap react independently to the applied field. For the "fused" sample, however, shielding

currents flow between the cylinder and the cap, leading unambiguously to better shielding at the closed extremity. This confirms the beneficial effect introduced by the superconducting joint.

V. Conclusion

The aim of the present work was to examine and understand the influence of a cap on the shielding properties for various semi-closed tubular superconducting samples. When the cap and the tube are separated by a non-superconducting joint or a small air gap, an improvement of the shielding volume can be achieved when the magnetic field is axial. The use of a thicker cap (or several caps) was shown to enhance the shielding factor inside the tube. For the transverse configuration, a cap with a small air gap leads to only a marginal improvement of the shielding factor at the extremity of the tube. The "adjusted" configuration, where a part of the air gap is oriented at 90° to the applied field, was found to yield a perceptible increase of the shielding factor, but only at low magnetic field. The configuration where the tube wall and the cap are grown in the same process clearly exhibits the best shielding properties in transverse field. This underlines the importance of using vessel-shaped shields [34, 41] and, more generally, of achieving superconducting joints between the superconducting components. In addition to the Buffer-Aided Top Seeded Melt Growth presented in this paper, multi-seeding [24] and the creation of artificially engineered boundaries [42-45] allowing high currents through melt-textured monoliths are also very promising approaches. In this case, the quality of the shielding would depend on the quality of the maximum current across such an artificial superconducting joint, which would need to be probed first through measurement of the transport critical current or electrical resistance [42-45]. Progress in this challenging area is expected to lead to significant advances in the development of efficient superconducting shields for high magnetic fields.

References

[1] J. Claycomb "Magnetic shields," in *Applied Superconductivity: Handbook on Devices and Applications*, vol. 1, Seidel P, Ed. Wiley, 1999, pp. 780-806.

[2] P. Arpaia, A. Ballarino, G. Giunchi, and G. Montenero, "MgB_2 cylindrical superconducting shielding for cryogenic measurement applications: a case study on DC current transformers," *Journal of Instrumentation,* vol. 9, no. 4, Apr. 2014, Art. no. P04020.

[3] A. Bergen, H. J. van Weers, C. Bruineman, M. M. J. Dhallé, H. J. G. Krooshoop, H. J. M. ter Brake, K. Ravensberg, B. D. Jackson, and C. K. Wafelbakker, "Design and validation of a large-format transition edge sensor array magnetic shielding system for space application," *Rev. Sci. Instrum*., vol. 87, no. 10, Oct. 2016, Art. no. 105109.

[4] C. Gu, S. Chen, T. Pang, and T.-M. Qu, "Experimental realization of open magnetic shielding," *Appl. Phys. Lett*. vol. 110, 2017, Art. no. 193505.

[5] D. Jiles, *Introduction to Magnetism and Magnetic Materials*, 3rd Edition*,* CRC Press, Taylor and Francis, 2015.

[6] D. Barna "High field septum magnet using a superconducting shield for the future circular collider," *Phys. Rev. Accel. Beams*, vol. 20, 2017, Art. no. 041002.

[7] K. G. Capobianco-Hogan *et al.,* "A magnetic field cloak for charged particle beams," *Nucl. Instrum. Methods. Phys. Res. A* vol. 877, pp. 149-156, 2018.

[8] M. Statera, I. Balossinoa, L. Barion, G. Ciullo, M. Contalbrigo, P. Lenisa, M. M .Lowry, A. M. Sandorfi, G. Tagliente, "A bulk superconducting MgB_2 cylinder for holding transversely polarized targets," *Nucl. Instrum. Methods. Phys. Res. A,* vol. 882, pp. 17-21, , Feb. 2018.

[9] J. F. Fagnard, S. Elschner, J. Bock, M. Dirickx, B. Vanderheyden, and P. Vanderbemden, "Shielding efficiency and E(J) characteristics measured on large melt cast Bi-2212 hollow cylinders in axial magnetic fields," *Supercond. Sci. Technol.*, vol. 23, no. 9, Aug. 2010, Art. no. 095012.

[10] J. J. Rabbers, M. P. Oomen, E. Bassani, G. Ripamonti, and G. Giunchi, "Magnetic shielding capability of MgB_2 cylinders," *Supercond. Sci. Technol.*, vol. 23, no. 12, Oct. 2010, Art. no. 125003.

[11] L. Gozzelino, R. Gerbaldo, G. Ghigo, F. Laviano, A. Agostino, E. Bonometti, M. Chiampi, A. Manzin, and L. Zilberti, "DC Shielding Properties of Coaxial MgB_2/Fe Cups," *IEEE Trans. Appl. Supercond*., vol. 23, no. 3, June 2013, Art. no. 8201305.

[12] G. Giunchi, D. Barna, H. Bajas, K. Brunner, A. Német, and C. Petrone, "Relaxation Phenomena in a Long MgB_2Tube Subjected to Transverse Magnetic Field, at 4.2 K" *IEEE Trans. Appl. Supercond.*, vol. 28, no. 4, June 2018, Art. no. 6801705.

[13] L. Wéra, J.-F. Fagnard, D. K. Namburi, Y. Shi, B. Vanderheyden, and P. Vanderbemden "Magnetic shielding above 1 T at 20 K with bulk, large grain YBCO tubes made by Buffer-aided Top Seeded Melt Growth," *IEEE Trans. Appl. Supercond.*, vol. 27, no. 4, June 2017, Art. no. 6800305.

[14] J. F. Fagnard, M. Dirickx, M. Ausloos, G. Lousberg, B. Vanderheyden, and P. Vanderbemden, "Magnetic shielding properties of high-T_c superconducting hollow cylinders: model combining experimental data for axial and transverse magnetic field configurations," *Supercond. Sci. Technol.*, vol. 22, no. 10, Aug. 2009, Art. no. 105002.

[15] L. Tomkow, M. Ciszek, and M. Chorowski, "Combined magnetic screen made of Bi-2223 bulk cylinder and YBCO tape rings—Modeling and experiments," *J. Appl. Phys.*, vol. 117, no. 4, 2015, Art. no. 043901.

[16] P.T. Yang, W. M. Yang, and J. L. Chen, "Fabrication and properties of single domain GdBCO superconducting rings by a buffer aided Gd+011 TSIG method" *Supercond. Sci. Technol.*, vol. 30, no. 8, Aug. 2017, Art. no. 085003.

[17] L. Gozzelino, R. Gerbaldo, G. Ghigo, F. Laviano, M. Truccato, and A. Agostino, "Superconducting and hybrid systems for magnetic field shielding," *Supercond. Sci. Technol.*, vol. 29, no. 3, Jan. 2016, Art. no. 034004.

[18] L. Gozzelino, R. Gerbaldo, G. Ghigo, F. Laviano, and M. Truccato, "Comparison of the Shielding Properties of Superconducting and Superconducting/Ferromagnetic Bi- and Multi-layer Systems," *Journal of Superconductivity and Novel Magnetism*, vol. 30, no. 3, pp 749–756, March 2017.

[19] L. Wéra, J. F. Fagnard, G. A. Levin, B. Vanderheyden, and P. Vanderbemden, "Magnetic Shielding With YBCO Coated Conductors: Influence of the Geometry on Its Performances," *IEEE Trans. Appl. Supercond.*, vol. 23, no. 3, Jun. 2013, Art. no. 8200504.

[20] Ł. Tomków, M. Ciszek, and M. Chorowski, "Frequency Effect on Shielding Quality of Closed Superconducting Magnetic Shields Made of Superconducting Tapes," *IEEE Trans. Appl. Supercond*., vol. 26, no. 3, April 2016, Art. no. 0602204.

[21] J. Kvitkovic, D. Davis, M. Zhang, and S. Pamidi, "Magnetic Shielding Characteristics of Second Generation High Temperature Superconductors at Variable Temperatures Obtained by Cryogenic Helium Gas Circulation," *IEEE Trans. Appl. Supercond.*, vol. 25, no. 3, Jun. 2015, Art. no. 8800304.

[22] J. Souc, M. Solovyov, F. Gömöry, J. Prat-Camps, C. Navau, and A. Sanchez "A quasistatic magnetic cloak," *New J. Phys*. vol. 15, May 2013, Art. no. 053019.

[23] K. Seo, S. Nishijima, K. Katagiri, T. Okada, "Evaluation of solders for superconducting magnetic shield," *IEEE Trans. Magn.*, vol. 27, no. 2, pp. 1877-1880, March 1991.

[24] Y. Shi, J. H. Durrell, A. R. Dennis, K. Huang, D. K. Namburi, D. Zhou and D. A. Cardwell, "Multiple seeding for the growth of bulk GdBCO–Ag superconductors with single grain behaviour", *Supercond. Sci. Technol.*, vol. 30, no. 1, Jan. 2017, Art. no. 015003.

[25] S. Nariki, H. Teshima, and M. Morita, "Performance and applications of quench melt-growth bulk magnets," *Supercond. Sci. Technol.*, vol. 29, no. 3, Jan. 2016, Art. no. 034002.

[26] S. Denis, M. Dirickx, P. Vanderbemden, M. Ausloos, and B. Vanderheyden, "Field penetration into hard type-II superconducting tubes: effects of a cap, a non-superconducting joint, and non-uniform

superconducting properties," *Supercond. Sci. Technol.*, vol. 20, no. 5, pp. 418-427, May 2007.

[27] E. H. Brandt, "Superconductor disks and cylinders in an axial magnetic field. I. Flux penetration and magnetization curves," *Phys. Rev. B.*, vol. 58, no. 10, Sept. 1998, pp. 6506–6521.

[28] L. Wéra, J. F. Fagnard, K. Hogan, B. Vanderheyden, and P. Vanderbemden, "Magnetic Shielding with Bulk High Temperature Superconductors: Improvement of the Shielded Volume in Hollow Cylinders," in *Superconductivity: Applications Today and Tomorrow* M. Muralidhar, Ed., ed New York: Nova Science, 2016, pp. 95-114.

[29] K. Hogan, J. F. Fagnard, L. Wéra, B. Vanderheyden, and P. Vanderbemden, "Bulk superconducting tube subjected to the stray magnetic field of a solenoid, " *Supercond. Sci. Technol.*, vol. 31, no. 1, Jan. 2018, Art. no. 015001.

[30] M. D. Ainslie and H. Fujishiro, "Modelling of bulk superconductor magnetization," *Supercond. Sci. Technol.*, vol. 28, no. 5, March 2015, Art. no. 053002.

[31] E. Pardo and M. Kapolka, "3D magnetization currents, magnetization loop, and saturation field in superconducting rectangular prisms," *Supercond. Sci. Technol.*, vol. 30, no. 6, May 2017, Art. no. 064007.

[32] N. Devendra Kumar, Y. Shi, W. Zhai, A. R. Dennis, J. H. Durrell, and D. A. Cardwell, "Buffer Pellets for High-Yield, Top-Seeded Melt Growth of Large Grain Y–Ba–Cu–O Superconductors," *Cryst. Growth Des.*, vol. 15, no. 3, pp. 1472-1480, Jan. 2015.

[33] D. K. Namburi, Y. Shi, K. G. Palmer, A. R. Dennis, J. H. Durrell, and D. A. Cardwell, "Control of Y-211 content in bulk YBCO superconductors fabricated by a buffer-aided, top seeded infiltration and growth melt process," *Supercond. Sci. Technol.*, vol. 29, no. 3, p. 034007, Feb. 2016.

[34] https://www.can-superconductors.com/magnetic-shields.html

[35] D. Ruiz-Alonso, T. A. Coombs, and A. M. Campbell, "Computer modelling of high-temperature superconductors using an A–V formulation," *Supercond. Sci. Technol.*, vol. 17, no. 5, pp. S305-S310, May 2004.

[36] F. Grilli, S. Stavrev, Y. Le Floch, M. Costa-Bouzo, E. Vinot, I. Klutsch, G. Meunier, P. Tixador, and B. Dutoit, "Finite-element method modeling of superconductors: from 2-D to 3-D," *IEEE Trans. Appl. Supercond.* vol. 15, no. 1, pp. 17-25, March 2005.

[37] G.P. Lousberg, M. Ausloos, C. Geuzaine, P. Dular, P. Vanderbemden and B. Vanderheyden, "Numerical simulation of the magnetization of high-temperature superconductors: a 3D finite element method using a single time-step iteration," *Supercond. Sci. Technol.*, vol. 22, no. 5, May 2009, Art 055005.

[38] GetDP: A General Environment for the Treatment of Discrete Problems, [Online]. http://getdp.info/

[39] C. P. Bean, "Magnetization of Hard Superconductors," *Phys. Rev. Lett*., vol. 8, pp. 250-253, 1962.

[40] B. Cabrera, "The use of superconducting shields for generating ultra-low magnetic field regions and several related experiments," PhD Thesis, Stanford University, USA, 1975.

[41] A. Koike A., K. Hoshino, H. Kotaka, E. Sudoh, K. Katoh, and H. Ohta "Large Vessels of Bi Oxide Superconductor for Magnetic Shield" in: Hayakawa H., Koshizuka N. (eds) *Advances in Superconductivity IV*. Springer, Tokyo, 1992, pp 1065-1068.

[42] K. Salama and V. Selvamanickam, "Joining of high current bulk Y-Ba-Cu-O superconductors," *Appl. Phys. Lett*. vol. 60, no. 7, pp.898-900, Feb. 1992.

[43] R. A. Doyle, A. D. Bradley, W. Lo, D. A. Cardwell, and A. M. Campbell, Ph. Vanderbemden, and R. Cloots, "High field behavior of artificially engineered boundaries in melt-processed $YBa_2Cu_3O_{7-\delta}$," *Appl. Phys. Lett*. vol. 73, no. 1, pp. 117-119, 1998.

[44] S. Iliescu, X. Granados, T. Puig, and X. Obradors, "Growth mechanism of Ag-foil-based artificially superconducting joints of $YBa_2Cu_3O_7$ monoliths," *J. Mater. Res.* vol. 21, no. 10, pp. 2534-2541, Oct. 2006.

[45] K. Iida, T. Kono, T. Kaneko, K. Katagiri, N. Sakai, M. Murakami, and N. Koshizuka, "Joining of different Y–Ba–Cu–O blocks," *Physica C* vol. 402, no. 1-2, pp. 119-126, Feb. 2004.

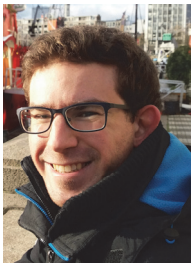

Laurent Wéra received his M.S. degree in aerospace engineering from the University of Liège, Belgium in 2011. Then he joined the SUPRATECS research group in the department of Electrical Engineering and Computer Science of the University of Liège as a teaching assistant and Ph.D. student. His Ph.D. thesis was dedicated to the experimental study of methods to increase the shielded volume in passive superconducting magnetic screens and was carried out under the supervision of Prof. Philippe Vanderbemden. He received his Ph.D. degree in September 2017. Then, he leaved the University of Liège and joined AMOS (Advanced Mechanical and Optical Systems) as an electromechanical engineer.

Jean-François Fagnard was born in Charleroi, Belgium, in 1977. He received the M.S. degrees in physics in 1998 and in physics engineering from the University of Liège, Belgium in 2000. In 2011, he received the Ph.D. degrees in engineering sciences from the University of Liège and in applied sciences from the Royal Military Academy, Brussels, Belgium.
From 2000 to 2007, he was Research Engineer and from 2007 to 2008, he was Teaching Assistant in the Department of Electrical Engineering and Computer Science at the University of Liège, Belgium. From 2008 to 2012, he was Research Engineer with the Royal Military Academy, Belgium. In 2013 he was a Research Associate for 6 months with the University of Cambridge, United Kingdom. He is now Research Associate with the Department of Electrical Engineering and Computer Science at the University of Liège, Belgium.
His main research interests are magnetic and transport properties of high-temperature superconductors for engineering applications (magnetic energy storage, magnetic shielding, crossed field effect) and include also the properties of other materials such as colossal magneto-resistive (CMR) compounds, magnetocaloric materials as well as the study of flash sintering in ceramic materials.

Kevin Hogan was born in Liège, Belgium in 1990. He received the M.S. degree in electrical engineering from the University of Liege, Liege, Belgium, in 2013, and the Ph.D. degree in engineering, under the supervision of P. Vanderbemden, from the Department of Electrical Engineering and Computer Science, University of Liege, in 2018. His Ph.D. dissertation was dedicated to passive magnetic shielding with bulk high-temperature superconductors under a non-uniform magnetic field. In 2016, he worked as a visiting student for three months in the Technology and Engineering Division at the Plasma Science and Fusion Center (PSFC) at the Massachusetts Institute of Technology (MIT).

Benoît Vanderheyden was born in Verviers, Belgium, in 1969. He received the M.S. degree in electrical engineering from the University of Liège, Belgium, in 1992. He received the M.S. and Ph.D. degrees in physics from the University of Illinois at Urbana-Champaign, IL, in 1994 and 1998, respectively. From 1998 to 2000, he was a postdoctoral fellow at the Niels Bohr Institute, Copenhagen, Denmark. He joined the Electrical Engineering and Computer Science Department of the University of Liège, Belgium, in 2000, where is now Full Professor. His research interests include modelling the electrical and magnetic properties of high-temperature superconductors and thin-film superconductor systems.

Devendra Kumar Namburi received M.Sc. and Ph.D. degrees in Physics from the University of Hyderabad, India. He worked as a post-doctoral researcher at the University of Liege, Belgium during 2012-2014. In 2014, he joined University of Cambridge as a Research Associate and has been working on bulk superconducting materials since then. His research interests are in applied high temperature superconductivity, including the processing of (RE)-Ba-Cu-O superconductors in bulk and thick film forms for various technological applications. His current work is focused in fabricating large single grains of (RE)-Ba-Cu-O superconductors by Top Seeded Melt Growth (TSMG) and Seeded Infiltration Growth (SIG) processes. He has authored over 30 technical papers and made presentations at over 20 international conferences. He was awarded with the prestigious Dr. D. C. Pavate Travel Bursary in 2017. Two of his papers were selected as Highlights of the journal *Superconductor Science and Technology* for the year 2017. Dr. Namburi has been a member of Sydney Sussex College, UK since 2017. In addition to the processing, Dr. Namburi has also developed skills in fabricating YBCO wires of short lengths using powder-in-tube method. Some of his goals include enhancing the field dependence of critical current densities, trapped magnetic fields of bulks, pulsed field magnetization, improving the shielding performance of cavities / thick films made out of these materials and develop expertise in the coated conductor technology.

David Cardwell studied Physics at the University of Warwick between 1980 and 1986, graduating with a BSc in 1983 and a PhD in 1987. He joined Plessey Research (Caswell) on completing his PhD, and prior to moving to Cambridge in 1992. He is currently Professor of Superconducting Engineering in the Department of Engineering, University of Cambridge, where he leads the Bulk Superconductivity Research Group on the processing and applications of bulk high temperature superconductors, which can be used to generate very high

magnetic fields, including the world record field on 17.6 T in a bulk superconductor set in 2014. He was appointed Head of the Cambridge Department of Engineering in October 2014. He was a founder member of the European Society of Applied Superconductivity (ESAS) in 1998 and has served as a Board member and Treasurer of the Society since 2007. He is an active board member of five international journals, including *Superconductor Science and Technology*, and has authored over 350 technical papers and patents and has given invited presentations at over 60 international conferences. He was awarded the PASREG prize for excellence in the processing of bulk superconductors in 2001, and collaborates widely around the world with academic institutes and industry. Professor Cardwell was elected to a Fellowship of the Royal Academy of Engineering in 2012 in recognition of his contribution to the development of superconducting materials for engineering applications. He was awarded a Sc.D. by the University of Cambridge in 2014 and an honorary D.Sc. by the University of Warwick in 2015. Professor Cardwell has been a Fellow of Fitzwilliam College since 1993 and has held various offices during this time, including Admissions Tutor for Sciences (2000-2013), Undergraduate Tutor (1995-2013) and Director of studies in Engineering (1996-1999).

Yunhua Shi received the B.Sc. in University of Science and Technology Beijing, China in 1984 and M.S. degrees in General Institute of Non-ferrous Metals in Beijing, China in 1989. She later received Ph.D. degree in Engineering Department, University of Cambridge in 2009. She has worked as Senior Research associate in Material research on LREBCO single grains and their applications from 2010 to date in Engineering Department, University of Cambridge. She has published over 120 papers.

Philippe Vanderbemden was born in 1973. He received the M.S. degree in electrical engineering and the Ph.D. degree from the University of Liege, Belgium, in 1995 and 1999 respectively. He was a Research Fellow and a Postdoctoral Researcher with the Belgian National Fund for Scientific Research (FNRS) and spent six months at the IRC in Superconductivity, University of Cambridge (UK). He was also a visiting researcher and at the National High Magnetic Field Laboratory, Tallahassee, FL (USA). In 2003, he joined the academic staff of the University of Liege, where he is a Full Professor in the Department of Electrical Engineering and Computer Science (Montefiore research unit). He has co-authored more than 120 research publications in conference proceedings and international journals. His research interests include magnetic and transport properties of high-temperature superconductors and related materials geared toward engineering applications, as well as high-sensitivity electrical and magnetic measurements.

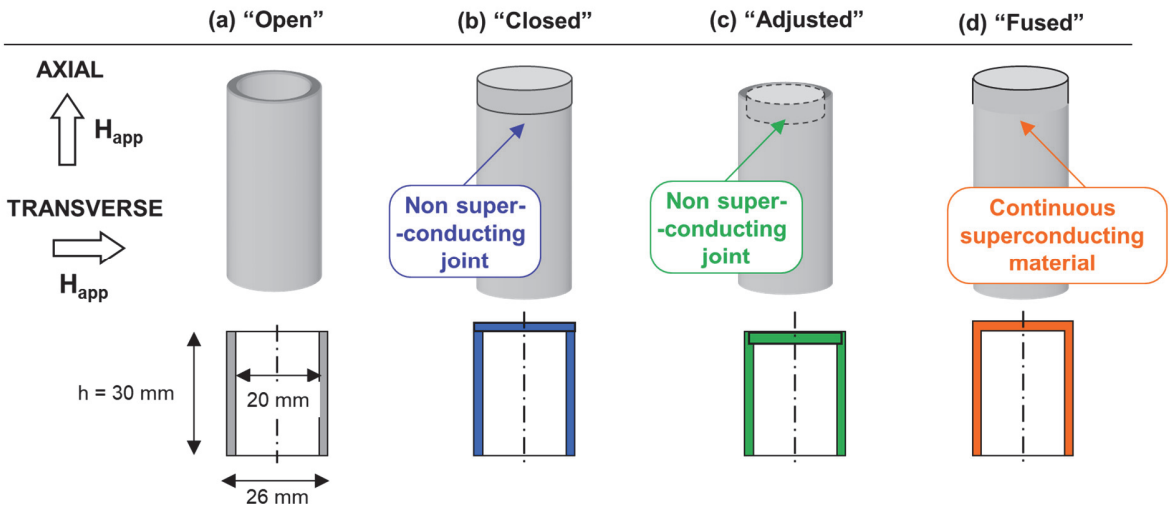

Fig. 1. Top: Schematic illustration of the "open", "closed", "adjusted" and "fused" configurations used in this paper. Bottom: Dimensions of the configurations modelled in transverse field. The details of the dimensions of the samples studied experimentally are given in Table I. The details of the dimensions of the modelled in both 2D and 3D are given in Table II.

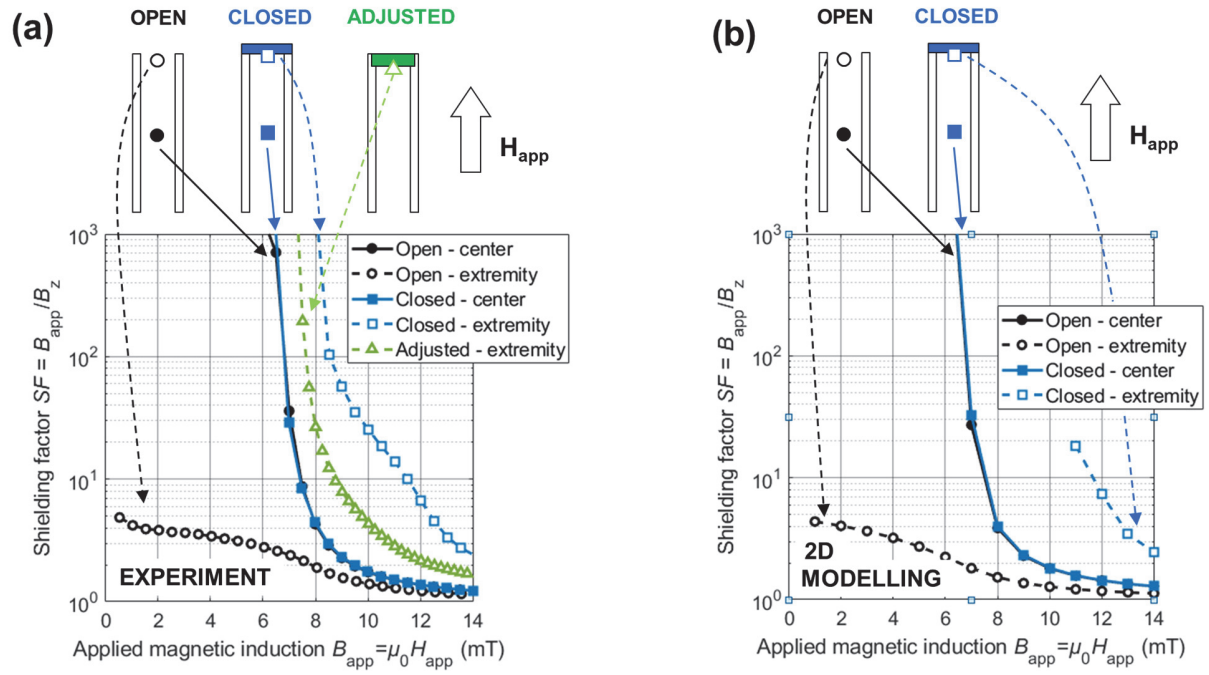

Fig. 2. (a) Experimental shielding factor $SF = B_{app}/B_{in}$ as a function of the magnetic field strength $B_{app} = \mu_0 H_{app}$ applied parallel to the axis of the tube for the "open", "closed" and "adjusted" configurations. The shielding factor is measured at the center of the tube (solid symbols) or at its extremity (open symbols). The exact dimensions of the samples studied experimentally are given in Table I. (b) Modelled shielding factor $SF = B_{app}/B_{in}$ as a function of the magnetic field strength $B_{app} = \mu_0 H_{app}$ applied parallel to the axis of the tube for the "open" and "closed" configurations. The exact dimensions of the modelled samples are given in Table II.

TABLE I
CHARACTERISTICS OF THE SAMPLES STUDIED EXPERIMENTALLY

	$Bi_2Sr_2Ca_2Cu_3O_{10}$ ceramic	Melt textured $YBa_2Cu_3O_7$
Length	80 mm	26.6 mm
Inner radius	10.5 mm	8 mm
Outer radius	12.25 mm	12.85 mm
Wall thickness	1.75 mm	4.85 mm
Cap radius	12.25 mm	12.85 mm
Cap thickness	2 mm	~ 2 mm
J_{c0} (77 K) tube	900 A/cm²	~ 1000 A/cm²
B_1 (77K) tube	3 mT	N/A (constant J_c)
J_{c0} (77 K) cap	750 A/cm²	~ 1000 A/cm²
B_1 (77K) cap	5 mT	N/A (constant J_c)

TABLE II
CHARACTERISTICS OF THE MODELLED SAMPLES

	2D Modelling Axial field	3D Modelling Transverse field
Length	80 mm	30 mm
Inner radius	10.5 mm	10 mm
Outer radius	12.25 mm	13 mm
Wall thickness	1.75 mm	3 mm
Cap radius for "closed" or "fused"	12.25 mm	13 mm
Cap radius for "adjusted"	N/A	10.5 mm
Cap thickness e_0	2 mm	2 mm
J_{c0} (77 K) tube	900 A/cm²	1000 A/cm²
B_1 (77K) tube	3 mT	N/A (constant J_c)
J_{c0} (77 K) cap	750 A/cm²	1000 A/cm²
B_1 (77K) cap	5 mT	N/A (constant J_c)

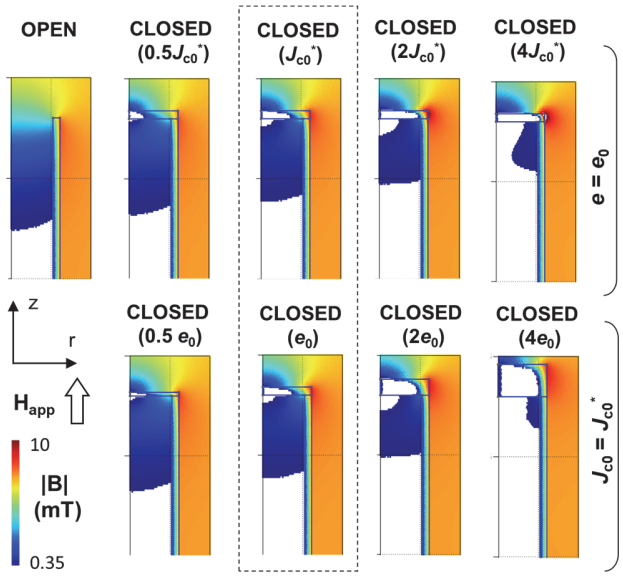

Fig. 3. Modelled distribution of magnetic flux density |B| for a long type-II superconducting tube subjected to an axial field $B_{app} = \mu_0 H_{app}$ = 7 mT. For each plot, the white area delimitates the zone for which the shielding factor is higher than 20. The framed plot shows the distribution of |B| for the nominal critical current density ($J_{c0} = J_{c0}^*$) and cap thickness (e_0). Top: constant thickness, increasing J_{c0}. Bottom: constant critical current density, increasing thickness. The exact dimensions of the modelled samples are given in Table II.

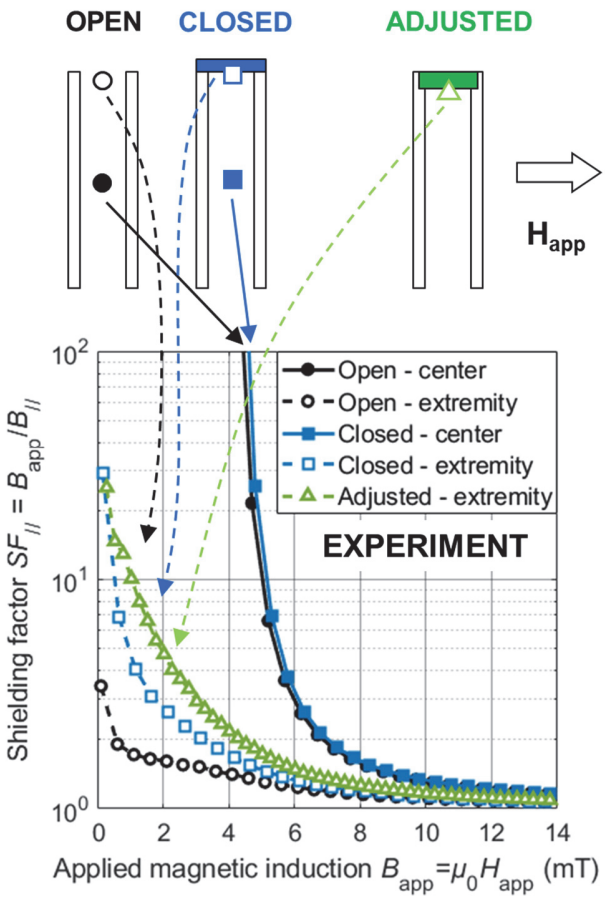

Fig. 4. Experimental shielding factor $SF = B_{app}/B_{\|}$ as a function of the magnetic field strength $B_{app} = \mu_0 H_{app}$ applied perpendicular to the axis of the tube for the "open", "closed" and "adjusted" configurations. $B_{\|}$ denotes the component of the magnetic flux density parallel to the direction of the applied field B_{app}. The shielding factor is measured at the center of the tube (solid symbols) or at its extremity (open symbols).

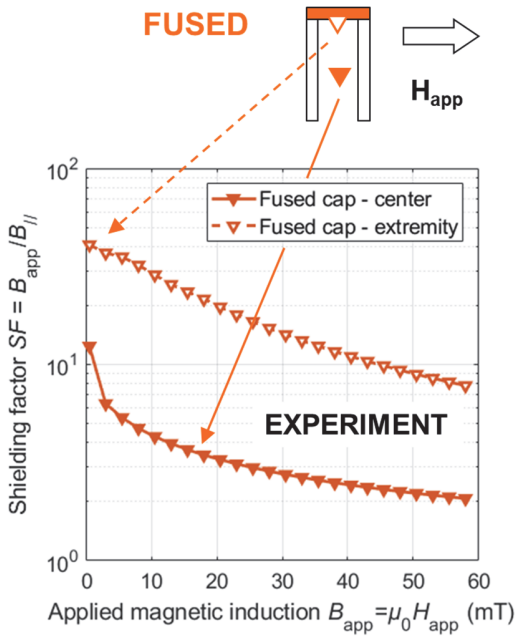

Fig. 5. Experimental shielding factor $SF = B_{app}/B_{\parallel}$ as a function of the magnetic field strength $B_{app} = \mu_0 H_{app}$ applied perpendicular to the axis of the tube for the "fused" configuration. $B_{\parallel}$ denotes the component of the magnetic flux density parallel to the direction of the applied field B_{app}. The shielding factor is measured at the center of the tube (solid symbols) or at its extremity (open symbols).

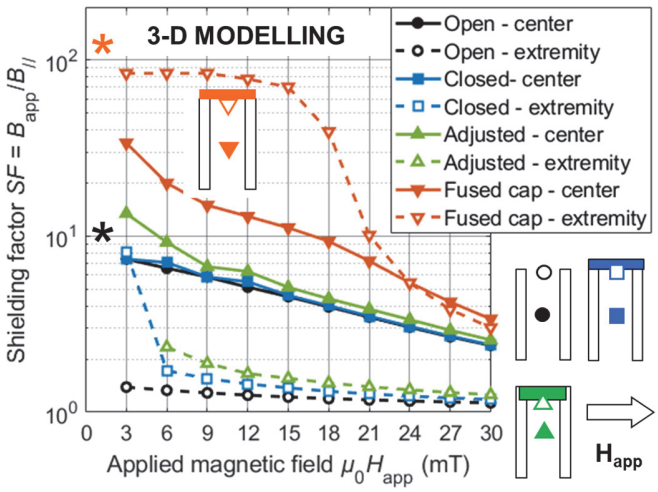

Fig. 6. Modelled shielding factor $SF = B_{app}/B_{\parallel}$ as a function of the magnetic field strength $B_{app} = \mu_0 H_{app}$ applied perpendicular to the axis of the tube for the 4 configurations shown in Fig. 1. $B_{\parallel}$ denotes the component of the magnetic flux density parallel to the direction of the applied field B_{app}. The shielding factor is modelled at the center of the tube (solid symbols) or at its extremity (open symbols). The stars refer to the theoretical shielding factor for a type-I superconductor of the same geometric dimensions. The exact dimensions of the modelled samples are given in Table II.

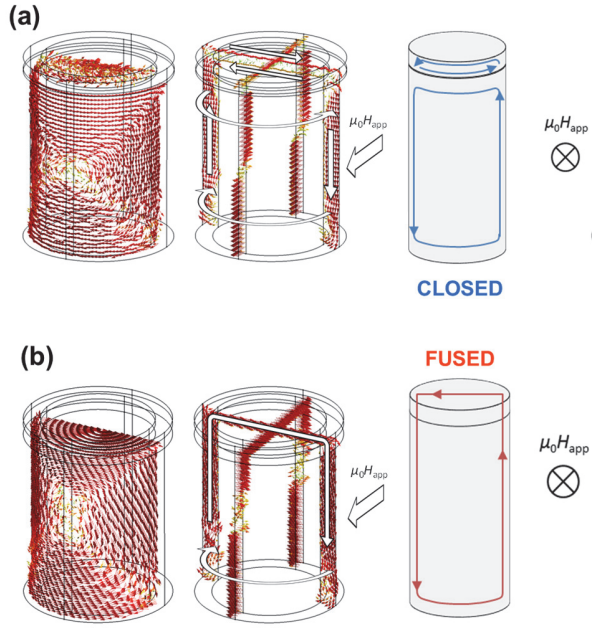

Fig. 7. Comparison of the modelled distribution of current density for the "closed" (a) and "fused" (b) configurations subjected to a transverse field $B_{app} = \mu_0 H_{app} = 30$ mT and schematic illustration of the shielding currents for both cases. The exact dimensions of the modelled samples are given in Table II.